Non-Overlapping Domain Decomposition Methods with Cross-Points and Padé Approximants for the Helmholtz Equation

Yassine Boubendir and Tadanaga Takahashi

1 Introduction

We present a new non-overlapping domain decomposition method (NDDM) based on the square-root transmission conditions and the utilization of an appropriate technique dealing with the so-called cross-points problem in the context of nodal finite element method (FEM). The square-root operator is localized using the Padé Approximants technique. In addition, we use a Krylov solver to accelerate the iterative procedure. Several numerical results are displayed to validate this new algorithm.

2 Model problem

Consider an obstacle S with a smooth boundary condition $\Gamma = \partial S$. We are solving for the scattered field u solution of the Helmholtz equation equipped with the Sommerfeld radiation condition

$$\begin{cases} \Delta u + k^2 u = 0 \text{ in } \mathbb{R}^2 \backslash \mathcal{S} \\ \partial_{\boldsymbol{n}_S} u = f \text{ on } \Gamma := \partial \mathcal{S} \\ \lim_{|\boldsymbol{x}| \to \infty} |\boldsymbol{x}|^{1/2} \left(\nabla u \cdot \frac{\boldsymbol{x}}{|\boldsymbol{x}|} - \mathrm{i}ku \right) = 0, \end{cases} \tag{1}$$

Yassine Boubendir
New Jersey Institute of Technology, 323 Dr Martin Luther King Jr Blvd, Newark, NJ 07102, e-mail: boubendi@njit.edu

Tadanaga Takahashi
New Jersey Institute of Technology, 323 Dr Martin Luther King Jr Blvd, Newark, NJ 07102, e-mail: tt73@njit.edu

where $\boldsymbol{n}_S$ indicates the outward unit normal to Γ, f is given in function of the plane wave $f = -\partial_{\boldsymbol{n}_S} e^{-ik\boldsymbol{d}\cdot\boldsymbol{x}}$, with $\boldsymbol{x} = (x_1, x_2) \in \mathbb{R}^2$ and $i = \sqrt{-1}$. The incidence angle $\boldsymbol{d}$ is normalized on the unit sphere $|\boldsymbol{d}| = 1$ and k denotes the wavenumber.
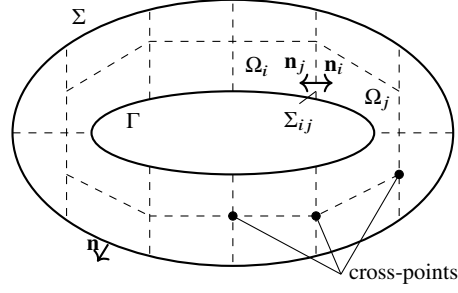
Fig. 1: Sketch of a non-overlapping domain decomposition of the domain Ω.

To solve problem (1), we truncate the original computational domain using an artificial interface Σ on which an absorbing boundary condition is posed, see Fig. 1. Therefore, problem (1) is reduced to the following system

$$\begin{cases} \Delta u + k^2 u = 0 \text{ in } \Omega \\ \partial_{\boldsymbol{n}} u = f \text{ on } \Gamma \\ \partial_{\boldsymbol{n}} u - iku = 0 \text{ on } \Sigma, \end{cases} \tag{2}$$

where $\boldsymbol{n}$ represents the normal derivative pointing outward from Ω.

3 Non-overlapping domain decomposition algorithm

The first step of this method consists of splitting the domain Ω into N_{dom} disjoint subdomains Ω_i, $i = 1, \ldots, N_{\text{dom}}$ such that:

- $\overline{\Omega} = \bigcup_{i=1}^{N_{\text{dom}}} \overline{\Omega}_i, \quad i = 1, \ldots, N_{\text{dom}}$
- $\Omega_i \cap \Omega_j = \emptyset, \quad \forall i \neq j, \quad i, j = 1, \ldots, N_{\text{dom}}$
- $\partial\Omega_i \cap \partial\Omega_j = \overline{\Sigma}_{ij} = \overline{\Sigma}_{ji}, \quad i, j = 1, \ldots, N_{\text{dom}}$.

We define $u_i, \Gamma_i, \Sigma_i, f_i$ to be their respective original definitions but restricted to $\overline{\Omega}_i$. Let $\mathbf{n}_i$ be the outward unit normal to $\partial\Omega_i$ and let Λ_i be the set of all indices of subdomains adjacent to Ω_i. Following Després' NDDM framework [5], we solve at each step $n + 1$ and for each subdomain $i = 1, \ldots, N_{\text{dom}}$, the local problem:

$$\begin{cases} \Delta u_i^{(n+1)} + k^2 u_i^{(n+1)} = 0 & \boldsymbol{x} \in \Omega_i \\ \partial_{\boldsymbol{n}_i} u_i^{(n+1)} = f_i & \boldsymbol{x} \in \Gamma_i \\ \partial_{\boldsymbol{n}_i} u_i^{(n+1)} - \mathrm{i} k u_i^{(n+1)} = 0 & \boldsymbol{x} \in \Sigma_i \\ \partial_{\boldsymbol{n}_i} u_i^{(n+1)} + \mathcal{B} u_i^{(n+1)} = g_{ij}^{(n)} & \boldsymbol{x} \in \Sigma_{ij} : j \in \Lambda_i, \end{cases} \qquad (3)$$

where $g_{ij}^{(n)}$ represent the transmitting quantities along the common interfaces defined by

$$g_{ij}^{(n)} = -\partial_{\boldsymbol{n}_j} u_j^{(n)} + \mathcal{B} u_j^{(n)} = 2\mathcal{B} u_j^{(n)} - g_{ji}^{(n-1)}. \qquad (4)$$

Several methods have been proposed in the past regarding the choice of the operator $\mathcal{B}$ in order to improve the convergence of the Després NDDM [2, 3, 4, 6, 8]. In this paper, we are interested in the following transmission operator

$$\mathcal{B}^{\mathrm{sq}, \varepsilon} u = -\mathrm{i} k \sqrt{1 + \mathrm{div}_{\mathcal{S}} \left(\frac{1}{k_\varepsilon^2} \nabla_{\mathcal{S}} \right)} u, \qquad (5)$$

where $\mathrm{div}_{\mathcal{S}}$ and $\nabla_{\mathcal{S}}$ represent the surface divergence and surface gradient of a surface $\mathcal{S}$, respectively, ε is a parameter which may depends on $\mathcal{S}$, and $k_\varepsilon = k + \mathrm{i}\varepsilon$ is its corresponding complexified wavenumber. Operator (5) is non-local but it can be localized using Padé approximants. The approximate square-root transmission operator of order N_{p} has the form

$$\mathcal{B}^{N_{\mathrm{p}}, \alpha, \varepsilon} u_i = -\mathrm{i} k \left(C_0 u_i + \sum_{\ell=1}^{N_{\mathrm{p}}} A_\ell \, \mathrm{div}_{\mathcal{S}} \left(\frac{1}{k_\varepsilon^2} \nabla_{\mathcal{S}} \varphi_{i,\ell} \right) \right), \qquad (6)$$

where the auxiliary unknowns $\varphi_{i,\ell}$ for $\ell = 1, \ldots, N_{\mathrm{p}}$ satisfy

$$\left(1 + B_\ell \, \mathrm{div}_{\mathcal{S}} \left(\frac{1}{k_\varepsilon^2} \nabla_{\mathcal{S}} \right) \right) \varphi_{i,\ell} = u_i. \qquad (7)$$

The C_0, A_ℓ, B_ℓ are complex Padé coefficients depending on a branch cut rotation parameter α. We refer to [2] for the details of this operator.

4 Nodal FEM-NDDM and the cross-points problem

The algorithm developed in [4] is based on the modification of the Padé transmission conditions introduced in [2]. The main goal of these modified conditions resides in reducing the cost of local problems because of the resolution of a series of equations on the artificial interfaces related to the auxiliary functions $\varphi_{i,\ell}$ (7) that are coupled to each local problem. In addition, this modification [4] leads to transmission conditions where the transmitting operator $\mathcal{B}$ is a scalar. In this case, it is possible to use the

approach dealing with the so-called *cross-points problem* developed for nodal FEM-NDDM [3]. The main idea of this approach consists of preserving the finite element equations at the level of these points, i.e., of taking a common value for the degree of freedom located on the nodes at the junction of several subdomains. The novelty of the method presented here consists of effectively extending this technique to the original Padé algorithm [2], i.e, in the case where the transmitting operator $\mathcal{B}$ is given by (6). Cross-points are corner nodes shared by multiple domains. The remainder of this section describes the steps of the nodal FEM-NDDM in [1, 3] adapted to (6)-(7).

Let $\mathcal{T}^h$ and X^h be, respectively, a global, non-degenerate triangular mesh of Ω and its associated $\mathbb{P}_1$-continuous finite element space. The discrete formulation of problem (2) is defined as follows

$$a_\Omega\left(u^h, v^h\right) = Lv^h, \qquad u^h \in X^h, \quad \forall v^h \in X^h \tag{8}$$

where

$$\begin{aligned}
a_\Omega\left(u^h, v^h\right) &:= \int_\Omega \left(\nabla u^h \cdot \nabla v^h - k^2 u^h v^h\right) \mathrm{d}\Omega - \mathrm{i}k \int_\Sigma u^h v^h \, \mathrm{d}\Sigma \\
Lv^h &:= \int_\Gamma f v^h \, \mathrm{d}\Sigma
\end{aligned} \tag{9}$$

and u^h is the FEM solution. Consider now the discrete solution to the local problem (3). Let $\mathcal{T}_i^h$ and X_i^h be, respectively, a non-degenerate triangular mesh of Ω_i and its associated $\mathbb{P}_1$-continuous finite element space which conforms to the global mesh. The discrete form of (3) with the Padé square root operator is

$$u_i^h \in X_i^h, \quad \forall v_i^h \in X_i^h$$

$$\begin{cases}
a_i(u_i^h, v_i^h) + \displaystyle\sum_{\ell=1}^{N_\mathrm{p}} p_{i,\ell}(\varphi_{i,\ell}^h, v_i^h) = L_i(v_i^h) \\
q_i(u_i^h, v_i^h) + r_{i,\ell}(\varphi_{i,\ell}^h, v_i^h) = 0 \quad \forall \ell = 1, \ldots, N_\mathrm{p},
\end{cases} \tag{10}$$

where

$$a_i(u_i, v_i) = \int_{\Omega_i} (\nabla u_i \cdot \nabla v_i - k^2 u_i v_i)\mathrm{d}x - \mathrm{i}k \int_{\Sigma_i} u_i \, v_i \mathrm{d}s - \mathrm{i}kC_0 \sum_{j \in \Lambda_i} \int_{\Sigma_{ij}} u_i v_i \mathrm{d}s \tag{11}$$

$$p_{i,\ell}(\varphi_{i,\ell}, v_i) = \sum_{j \in \Lambda_i} A_\ell \frac{\mathrm{i}k}{k_\varepsilon^2} \int_{\Sigma_{ij}} \nabla_{\Sigma_{ij}} \varphi_{i,\ell} \cdot \nabla_{\Sigma_{ij}} v_i \, \mathrm{d}s \tag{12}$$

$$q_i(u_i, v_i) = \sum_{j \in \Lambda_i} \int_{\Sigma_{ij}} u_i v_i \, \mathrm{d}s \tag{13}$$

$$r_{i,\ell}(\varphi_{i,\ell}, v_i) = -\sum_{j \in \Lambda_i} \int_{\Sigma_{ij}} \varphi_{i,\ell} v_i \, \mathrm{d}s + \frac{B_\ell}{k_\varepsilon^2} \int_{\Sigma_{ij}} \nabla_{\Sigma_{ij}} \varphi_{i,\ell} \cdot \nabla_{\Sigma_{ij}} v_i \mathrm{d}s \tag{14}$$

$$L_i(v_i) = \int_{\Gamma_i} f_i\, v_i\, \mathrm{d}s + \sum_{j \in \Lambda_i} \int_{\Sigma_{ij}} g_{ij} v_i\, \mathrm{d}s. \tag{15}$$

with $\varphi_{i,\ell} = 0$ on $\partial\Sigma_{ij}$. The method proposed here consist in relating the discrete original problem with the discrete local problems. We start by classifying the nodes of our mesh as one of the following:

- Independent: these nodes are interior to Ω_i, Σ_i, and Γ_i.
- Shared: these nodes are interior to Σ_{ij}.
- Cross-points: these are points where any of the curves Γ_i, Σ_{ij}, or Σ_i meet.

Any discrete local test function $v_i^h \in X_i^h$ can be decomposed as follows:

$$v_i^h = v_{iI}^h + \sum_{j \in \Lambda_i} v_{ij}^h + v_c^h, \tag{16}$$

where v_{iI}^h is supported only on independent nodes, v_{ij}^h is supported only on shared nodes, and v_c^h is supported only on cross-points. Let us introduce the broken space X_B^h defined as the span of the function

$$v^h = \sum_{i=1}^{N_{dom}} \left(v_{iI}^h + \sum_{j \in \Lambda_i} v_{ij}^h \right) + v_c^h, \tag{17}$$

see [1, 3] for more details. We are also defining the series of functions $(\varphi_{i,1}^h, ..., \varphi_{i,N_p}^h)$ in the space $(\Phi_i^h)^{N_p}$ where Φ_i^h represents a subspace of X_i^h supported only on the shared nodes. Finally, using conditions (4), the decompositions (16) and (17), and following a similar derivation to the algorithm described in [1], we can see that problem (8) is reduced to solving the following system

$$\left.\begin{aligned}
a_i\left(u_{iI}^h + \sum_{j \in \Lambda_i} u_{ij}^h + u_c^h, v_{iI}^h\right) &= L_i(v_{iI}^h), \quad \forall v_{iI}^h \in X_i^h \\
a_i\left(u_{iI}^h + \sum_{j \in \Lambda_i} u_{ij}^h + u_c^h, v_{ij}^h\right) + \sum_{\ell=1}^{N_p} p_{i,\ell}(\varphi_{i,\ell}^h, v_{ij}^h) &= L_i(v_{ij}^h), \\
q_i(u_{ij}^h, v_{ij}^h) + r_{i,\ell}(\varphi_{i,\ell}^h, v_{ij}^h) = 0, \quad \forall \ell = 1, \ldots, N_p, \\
\forall v_{ij}^h \in X_i^h, \quad j \in \Lambda_i
\end{aligned}\right\}, i = 1, \ldots, N_{dom}$$

$$\sum_{i=1}^{N} a_i\left(u_{iI}^h + \sum_{j \in \Lambda_i} u_{ij}^h + u_c^h, v_c^h\right) = \sum_{i=1}^{N} L_i(v_c^h) \quad \forall v_c^h \in X_c^h,$$

$$\tag{18}$$

and this system can be put in the matrix form (with N subdomains) as follows

$$
\begin{bmatrix}
A_{11} & P_1 & & & & A_{1c} \\
Q_1 & R_1 & & & & 0 \\
& & \ddots & & & \vdots \\
& & A_{NN} & P_N & A_{Nc} \\
& & Q_N & R_N & 0 \\
A_{c1} & 0 & \dots & A_{cN} & 0 & A_{cc}
\end{bmatrix}
\begin{bmatrix}
\boldsymbol{u_1} \\
\boldsymbol{\varphi_1} \\
\vdots \\
\boldsymbol{u_N} \\
\boldsymbol{\varphi_N} \\
\boldsymbol{u_c}
\end{bmatrix}
=
\begin{bmatrix}
\boldsymbol{g_1} \\
\boldsymbol{0} \\
\vdots \\
\boldsymbol{g_N} \\
\boldsymbol{0} \\
\boldsymbol{g_c}
\end{bmatrix}
\tag{19}
$$

with the quantities g_i being computed from the equation (15) where g_{ij} is updated on Σ_{ij} at each step $(n+1)$ as follows

$$
g_{ij}^{(n+1)} = -g_{ji}^{(n)} - 2ik \left(C_0 u_i^{(n+1)} + \sum_{\ell=1}^{N_p} A_\ell \, \mathrm{div}_{\Sigma_{ij}} \left(\frac{1}{k_\varepsilon^2} \nabla_{\Sigma_{ij}} \varphi_{i,\ell} \right) \right),
\tag{20}
$$

where $\varphi_{i,\ell}$ are the auxiliary functions corresponding to the solution $u_i^{(n+1)}$. The system (19) is similar to the one numbered (21) in [3] obtained in the case where $\mathcal{B}$ is a scalar. We use the same procedure (based on a Schur complement) described in [3] to deal with (19). For that, one needs to change the notations in this description and consider that each blocks A_{ii} is composed by the sub-blocks A_{ii}, P_i, Q_i, and R_i.

5 Numerical Results

This section is devoted to validating the proposed method through numerical simulations. We generate a triangular mesh controlled by 2 parameters: wavelength λ and points per wavelength n_λ. We use both a Krylov subspace solver (Orthodir) and successive approximation (Jacobi) methods to solve the iteration operator [7]. Because its performance, we choose to compare our new method (19) with the one called evanescent mode damping algorithm (EMDA) [3] which consists of choosing $\mathcal{B} = -ik(1 + i\mathcal{X})$. We evaluate the performance based on the number of iterations until *convergence* (initial residue decreases by a factor of 10^{-6}). For the Padé param-
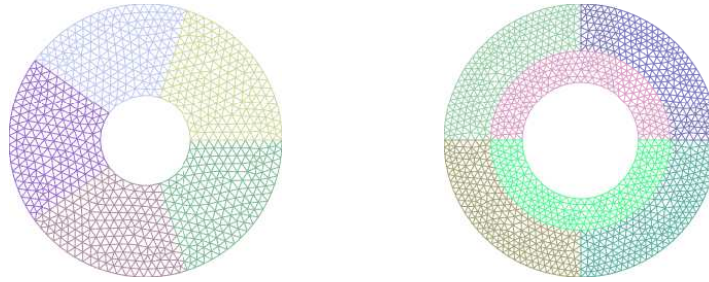
Fig. 2: Geometries used for the numerical simulation: pie (left) and layered (right) configurations.

eters, we chose [2] $\alpha = \pi/4$ and $\varepsilon = 0.6k^{1/3}$. For the EMDA, we chose $\mathcal{X} = 1/2$. These simulations are performed on the 2 geometries shown in Fig. 2.

In the pie configuration (left of Fig. 2), the annulus is split radially into N_{dom} equal subdomains. The inner radius is fixed $r_1 = 1$ and the outer radius varies with frequency $r_2 = r_1 + 2\pi/k$. In the first experiment, we fixed $N_{\text{dom}} = 5$, $k = \pi$, varied $n_\lambda = 12, 16, 20, 24$, and Padé orders $N_{\text{p}} = 1, 2, 4, 8$. Table 1 shows the obtained results. In the second experiment, we determine how the wavenumber affects the

Table 1: Number of iterations till convergence with respect to points per wavelength n_λ

	Jacobi					Orthodir				
n_λ	EMDA	Padé1	Padé2	Padé4	Padé8	EMDA	Padé1	Padé2	Padé4	Padé8
12	105	33	25	25	25	28	18	15	14	14
16	136	44	28	24	24	32	20	17	14	14
20	159	52	34	23	23	35	22	18	15	15
24	192	63	42	23	23	38	24	20	16	15

convergence rate. Table 2 displays the results for fixed $N_{\text{dom}} = 5$, $n_\lambda = 16$ and wavenumber varied $k = \pi, 2\pi, 3\pi, 4\pi$. In the third experiment, we varied the number of subdomains $N_{\text{dom}} = 2, 4, 6, 12$ with fixed $k = \pi$ and $n_\lambda = 16$. These results are summarized in Table 3.

Table 2: Number of iterations till convergence with respect to wavelength k

	Jacobi					Orthodir				
k	EMDA	Padé1	Padé2	Padé4	Padé8	EMDA	Padé1	Padé2	Padé4	Padé8
π	136	44	28	24	24	32	20	17	14	14
2π	124	40	25	22	22	29	19	16	14	14
3π	127	41	26	24	24	30	20	16	15	15
4π	120	39	25	24	24	29	19	16	15	15

Table 3: Number of iterations till convergence with respect to number of subdomains N_{dom}

	Jacobi					Orthodir				
N_{dom}	EMDA	Padé1	Padé2	Padé4	Padé8	EMDA	Padé1	Padé2	Padé4	Padé8
2	136	44	28	17	17	20	14	13	12	11
4	137	44	27	20	20	29	18	15	13	13
6	139	44	28	25	25	32	20	17	15	15
12	139	67	54	50	49	39	28	24	23	23

Table 4: Results for the cross-point configuration experiments

	Jacobi			Orthodir				Jacobi			Orthodir		
n_λ	EMDA	Padé2	Padé4	EMDA	Padé2	Padé4	k	EMDA	Padé2	Padé4	EMDA	Padé2	Padé4
12	110	60	59	36	24	24	π	123	70	68	40	25	25
16	123	70	68	40	25	25	2π	115	44	44	42	31	31
20	144	76	73	43	27	26	3π	110	53	53	45	37	37
24	165	81	79	46	29	27	4π	165	56	56	46	42	42

The layered configuration (right of Fig. 2) is a six-domain annulus in which the radii $r_1 = 1, r_2 = 3$ and N_{dom} are fixed. For this geometry, we first varied $n_\lambda = 12, 16, 20, 24$ with fixed $k = \pi$. We then tested several wavenumbers $k = \pi, 2\pi, 3\pi, 4\pi$ with fixed $n_\lambda = 16$. All the obtained results are listed in Table 4.

These tests demonstrate the effectiveness of the combination of the square root transmission operator, localized using Padé approximants, with the treatment of the cross-points. We observe stability and consistency in terms of convergence, in particular when the Krylov solver Orthodir is applied.

References

1. Abderrahmane Bendali and Yassine Boubendir. Non-overlapping Domain Decomposition Method for a Nodal Finite Element Method. *Numerische Mathematik*, 103(4):515–537, June 2006.
2. Y. Boubendir, X. Antoine, and C. Geuzaine. A Quasi-Optimal Non-Overlapping Domain Decomposition Algorithm for the Helmholtz Equation. *J. Comput. Phys.*, 231(2):262–280, January 2012.
3. Y. Boubendir, A. Bendali, and M. B. Fares. Coupling of a Non-Overlapping Domain Decomposition Method for a Nodal Finite Element Method with a Boundary Element Method. *Int. J. Numer. Methods in Engrg.*, 73(11):1624–1650, March 2008.
4. Yassine Boubendir and Dawid Midura. Non-overlapping domain decomposition algorithm based on modified transmission conditions for the helmholtz equation. 75(6).
5. Bruno Desprès. *Méthodes De Décomposition de Domaine pour les Problemes De Propagation D'ondes en Régime Harmonique*. phdthesis.
6. Martin J. Gander, Frédéric Magoulès, and Frédéric Nataf. Optimized schwarz methods without overlap for the helmholtz equation. 24(1):38–60.
7. Y. Saad. *Iterative Methods for Sparse Linear Systems*. SIAM, 2nd ed edition.
8. Christiaan C. Stolk. A rapidly converging domain decomposition method for the helmholtz equation. 241:240–252.